TECHNICAL MEMORANDUM

264

User requirements for the assimilation of TRMM products in the ECMWF 4D Var system

J-F. Mahfouf, É. Gérard, V. Marécal,
M. Miller and R. Saunders

Research Department

November 1998

European Centre for Medium-Range Weather Forecasts
Europäisches Zentrum für mittelfristige Wettervorhersage
Centre européen pour les prévisions météorologiques à moyen

User requirements for the assimilation of TRMM products in the ECMWF 4D-Var system

By **Jean-François Mahfouf, Élisabeth Gérard, Virginie Marécal, Martin Miller and Roger Saunders**

Abstract

This report describes preliminary results on a EU-ESA funded contract (*EuroTRMM*) where the impact of TRMM (Tropical Rainfall Measuring Mission) data and products will be evaluated within the ECWMF four-dimensional variational (4D-Var) assimilation system. Two approaches for the assimilation of TRMM products are proposed: a direct assimilation of TMI brightness temperatures for total column water vapour and surface wind speed retrievals and a variational assimilation of satellite-derived rainfall rates provided by a synergetic algorithm. A 1D-Var assimilation of precipitation rates is illustrated using simulated observations and the ECMWF mass-flux convection scheme. The accuracy assessment of retrieved total column water vapour, surface wind speed and cloud water path using TMI brightness temperatures in a 1D-Var inversion is described. Rainfall rates produced by the ECMWF short-range forecasts and derived from SSM/I using a statistical regression (*Ferraro*, 1997) are compared in a preliminary study. From this comparison, recommendations are provided on the temporal and spatial scales of TRMM data for their assimilation in the ECMWF 4D-Var system and to evaluate the quality of medium-range forecasts.

1. Introduction

EuroTRMM is a 3-year EU-ESA funded project between various European organizations. It aims to examine the feasibility of the assimilation of precipitation derived from the satellite mission TRMM (Tropical Rainfall Measuring Mission) in the ECMWF 4D-Var system. This report describes the methodology to be developed at ECMWF for the assimilation of both satellite radiances and derived products. Emphasis is put on the consistency between temporal and spatial scales resolved by the ECMWF model and by the satellite observations.

The latent heat released in tropical rainfall plays a crucial role in driving the low-latitude atmospheric circulation. However, conventional rainfall measurements are scarce in the tropics. Satellite observation is thus the only effective way to provide continuous monitoring of precipitation events. The Tropical Rainfall Measuring Mission (TRMM) is the first satellite for earth observation to have on board a Precipitation Radar (PR), in association with microwave (TMI) and visible/infra-red (VIRS) imaging radiometers (*Simpson et al.*, 1996). Accurate measurements of satellite-derived rainfall rates expected from TRMM could be used in Numerical Weather Prediction (NWP) for improving the quality of operational analyses and forecasts. Indeed, one difficulty of most NWP models is their inability to produce realistic weather elements, such as clouds and precipitation, at the beginning of the forecast period. This "spin-up problem" corresponds to an imbalance of the hydrological cycle during the first hours of the forecast and is generally more pronounced in the tropics than in mid-latitudes.

Section 2 provides a review of recent methods developed to assimilate satellite rainfall rates in NWP models. A description of the ECMWF model and of the 4D-Var assimilation system is given in Sections 3 and 4. The methodology to be developed for the assimilation of TRMM products in the 4D-Var system is presented in Section 5. Preliminary results of a 1D-Var assimilation of simulated rainfall observations are described in Section 6. The accuracy of TMI retrievals for total column water vapour, wind speed and cloud liquid water is assessed in Section 7 and compared to SSM/I retrievals. For a case study, short-range forecasts of precipitation produced by the ECMWF model are compared with instantaneous rainfall rates derived from SSM/I in Section 8. Section 9 provides recommendations on TRMM data and products required in the ECMWF 4D-Var system and to evaluate the skill of model forecasts.

6-hour forecast). The background information valid at time t_0 summarizes all information used before that time. Superscripts -1 and T denote respectively matrix inverse and transpose. The superscript i denotes the time index.

The model state $x(t_i)$ is defined as:

$$x(t_i) = M(t_i, t_0)[x_0]$$

where M is the forecast model integrated from time t_0 to time t_i.

The minimization of the cost-function J is done through a descent algorithm (M1QN3 from INRIA (*Gilbert and Lemaréchal*, 1989)) which requires several computations of the gradient of J with respect to the initial state x_0. These computations are done using the adjoint technique, described in the Appendix B.

4.2 The incremental approach

The incremental 4D-Var (*Courtier et al.*, 1994) consists of computing the background trajectory and the departures (observations minus model) using the full non-linear model at high resolution including a full set of physical parametrizations, and minimizing the cost-function in a low resolution space for the increments at initial time using a tangent linear model $\mathbf{M}$ and its adjoint with a limited set of physical parametrizations.

Writing

$$x_0 = x_0^b + \delta x$$

and

$$H_i[x(t_i)] = H_i[x^b(t_i)] + \mathbf{H}_i \cdot \delta x(t_i)$$

with $\mathbf{H}_i$ the linearization of the observation operator H_i in the vicinity of the background x^b and:

$$\delta x(t_i) = \mathbf{M}(t_i, t_0) \cdot \delta x_0$$

the new cost-function becomes:

$$J(\delta x) = \frac{1}{2}(\delta x_0)^T \mathbf{B}^{-1}(\delta x_0) + \frac{1}{2}\sum_{i=0}^{n}(\mathbf{H}_i \cdot \delta x(t_i) - d_i)^T \mathbf{R}_i^{-1}(\mathbf{H}_i \cdot \delta x(t_i) - d_i)$$

with $d_i = y_i^o - H_i[x^b(t_i)]$ the innovation vector.

The optimum δx^a is added to the background x^b in order to provide the analysis x^a:

$$x^a = x^b + \delta x^a$$

As stated by *Courtier et al.* (1994), one can make two important remarks about this method

1) This formulation allows for simplifications of the tangent linear model and reduction of the control variable. In practice, the increments are computed at T63 resolution (about 200 km).

2) It is possible to take into account the non-linearities introduced by the physical processes by updating iteratively the trajectory in the vicinity of which the model is linearized.

In the current ECMWF operational 4D-Var, 2 external updates of the trajectory are performed. The first inner-loop minimization is performed through 50 iterations with an adiabatic tangent-linear model. The second minimization consists

of 20 iterations with a complete set of linear physical processes (*Rabier et al.*, 1997b). The time window is currently 6 hours and is planned to be extended in the future to 12 and 24 hours. The development of the adjoint of the semi-lagrangian time integration scheme is required to compute higher resolution increments at a reasonable computing cost.

5. METHODOLOGY FOR THE ASSIMILATION OF TRMM RAINFALL RATES

The physical initialization technique described in Section 2 for the assimilation of satellite rainfall rates in NWP models is expected to improve the ECWMF assimilation system when applied to TRMM products for the following reasons:

1) More reliable satellite-derived rainfall rates will be provided by TRMM (through better calibration and validation of the inverse algorithms)

2) The 4D-Var assimilation is a more optimal technique than previous analysis schemes (such as Optimum Interpolation) to extract and to use information contained in satellite observations.

3) Physical parametrizations in the ECMWF model for convection and clouds provide a more comprehensive description of the processes than simpler schemes (e.g. Kuo scheme for convection or diagnostic cloud schemes).

Two options are possible for the variational assimilation of TRMM rainfall rates.

A 1D-Var assimilation of SSM/I radiances has already been developed by *Phalippou* (1996) at ECMWF using the adjoint of a microwave radiative transfer model. This technique allows retrieval of total column water vapour, liquid water path and surface wind speed and is currently used to monitor the ECMWF forecasts. The radiative transfer model can be adapted to TMI frequencies for the retrieval of same quantities in non-rainy areas (since the microwave radiative transfer model does not describe scattering effects), as explained more precisely in Section 7.

The adjoint of moist physical processes (deep and shallow convection, grid-scale precipitation) allows the fitting of temperature and specific humidity profiles in order to match observed surface rainfall rates, as shown in a feasibility study by *Fillion and Errico* (1997). As a first stage, a 1D-Var assimilation using the adjoint of the ECMWF moist physics and observed rainfall rates will be performed. Rainfall rates could be provided by statistical regressions (e.g. *Ferraro*, 1997) or by other inversion techniques (combining TMI and VIRS informations). In this context, it is possible to use the existing framework of the 1D-Var satellite retrievals developed at ECMWF for TOVS and SSM/I radiances in order to get collocated first-guess profiles and background error statistics (*Andersson et al.*, 1993). The difficulty of this approach is the specification of observation errors for the satellite-derived rainfall rates, as well as bias corrections and quality control.

The second approach is the development of a coupled 1D-Var assimilation using both the physical parametrizations and the radiative transfer model. Specification of observation errors is easier than for the previous option (since they are mostly instrumental and representativeness errors). Optimal profiles of specific humidity and temperature are obtained from a minimization algorithm in order to match observed TMI brightness temperatures, given a background constraint. The coupling will take place through rainfall rate profiles. Indeed, moist physical parametrizations provide at each model time step a rainfall rate profile that can be used as an input for the radiative transfer model (if a drop size distribution of hydrometeors is specified). The current ECMWF microwave radiative transfer model needs to be adapted to scattering atmospheres before such approach is viable. A similar methodology has already been adopted by *Aonashi et al.* (1997) in a mesoscale model with promising results.

The 1D retrieved profiles will be introduced in the 4D-Var assimilation system in a way to be defined (direct profiles, total column water vapour). The next step is to perform for both approaches a 4D-Var assimilation to ensure the horizontal and temporal consistency of observations.

The proposed methodology could be developed using SSM/I data first, before being applied to TRMM products.

6. A 1D-VAR ASSIMILATION OF SURFACE RAINFALL RATES FROM SIMULATED OBSERVATIONS

A simple example describing a variational assimilation of rainfall rates (simulated observations) is presented in a one-dimensional framework, to illustrate how this problem can be solved using the adjoint versions of moist physical parametrizations.

An instantaneous precipitation rate P can be simulated by the non-linear moist physical parametrizations of the ECMWF model (deep cumulus convection and large scale condensation) given an atmospheric profile $x = (T, q, p_s)$, where $T(p)$ is temperature, $q(p)$ specific humidity and p_s surface pressure.

From TRMM products, an observed instantaneous rainfall rate P_o can be estimated with an associated observation error σ_o.

The 1D-Var assimilation consists in finding an optimum profile x which minimizes a distance between the model rainfall rate and a corresponding observation, given a background constraint provided by a 6-hour forecast profile x^b. The analysed profile minimizes the following cost-function:

$$J(x) = \frac{1}{2}(x - x^b)^T \mathbf{B}^{-1}(x - x^b) + \frac{1}{2}\left[\frac{P_o - P(x)}{\sigma_o}\right]^2$$

The covariance matrix of background errors $\mathbf{B}$ used in the operational ECMWF 4D-Var system has been computed by *Rabier et al.* (1997a) and *Bouttier et al.* (1997). The covariance coefficients are computed statistically using the NMC method (*Parrish and Derber*, 1992) from differences between 48-hour and 24-hour forecasts. An example of vertical profiles for standard deviation of temperature and specific humidity is given in Figure 1 for tropical conditions. As in the ECMWF analysis system, no cross-correlations between background error on specific humidity and temperature are considered. The use of "unbalanced" temperature background errors (*Bouttier et al.*, 1997) leads to rather small standard deviations over the vertical (about 0.8 K). The vertical distribution of standard deviation for specific humidity exhibits a maximum at level 26 (around 850 hPa), an exponential decrease above and lower values in the boundary layer. The reduction near the surface is a consequence of the low variability of humidity in the tropical boundary layer which is strongly constrained by the imposed sea surface temperature.

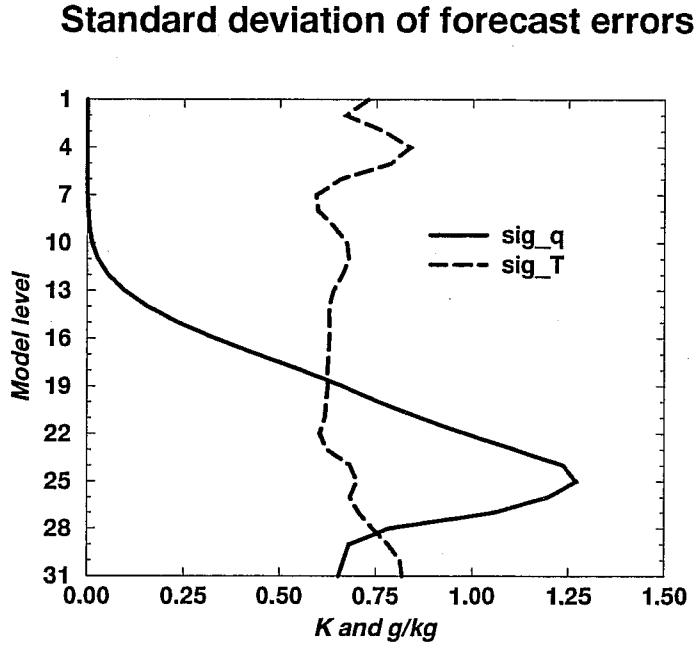

Figure 1: Vertical profile of standard deviation of forecast errors for temperature and specific humidity computed by Bouttier et al. (1997) for tropical atmospheres.

To find the minimum of the cost-function, its gradient with respect to x ($\nabla_x J$) must be computed. The adjoint technique is used to compute $\nabla_x J$ (see details in the Appendix B).

A preconditioning of the minimization can be done to improve the convergence. The matrix $\mathbf{B}$ is real symmetric, and can be decomposed in the following way:

$$\mathbf{B} = \mathbf{E}\Lambda\mathbf{E}^T$$

where $\mathbf{E}$ is the matrix of the eigenvectors of $\mathbf{B}$ displayed in columns and Λ the diagonal matrix of the eigenvalues of $\mathbf{B}$. This decomposition leads to the following change of variable:

$$v = \Lambda^{-\frac{1}{2}}\mathbf{E}^T(x - x^b)$$

The problem is then minimized in the v-space, and at the end of the minimization an inverse change of variable is performed:

$$x = x^b + \mathbf{E}\Lambda^{\frac{1}{2}}v$$

The gradient of the cost-function in the v-space is:

$$\nabla_v J = v + \Lambda^{\frac{1}{2}}\mathbf{E}^T\mathbf{P}^T\left[\frac{P_o - P(x)}{\sigma_o^2}\right]$$

The linear operator $\mathbf{P}^*$ is the adjoint of the physical parametrizations. This operator is the transpose of the Jacobian matrix of the partial derivatives of rainfall rates with respect to the input profile x:

$$\mathbf{P}^T = \left[\frac{\partial P}{\partial T_i}\ \frac{\partial P}{\partial q_i}\ \frac{\partial P}{\partial p_s}\right]$$

A set of preliminary experiments has been performed in order to demonstrate the feasibility of the 1D-Var method to assimilate satellite-derived rainfall rates. In the following, the cumulus convection parametrization is the ECMWF mass-flux scheme previously described and the minimization module is a limited memory quasi-newton (M1QN3 from INRIA).

An initial tropical profile x^b is taken from the ECMWF first-guess (6-hour forecast) at 1200 Z 08 January 1998 along the Equator (0°N,35°W). A simulated observation is created from the first-guess rainfall rate:

$$P_o = \alpha P^b$$

with a corresponding observation error, as proposed by *Fillion and Errico* (1997):

$$\sigma_o = 0.25 \cdot P^b$$

Results from two experiments where precipitation rate is respectively increased and decreased by 50 % with respect to the first-guess value are described.

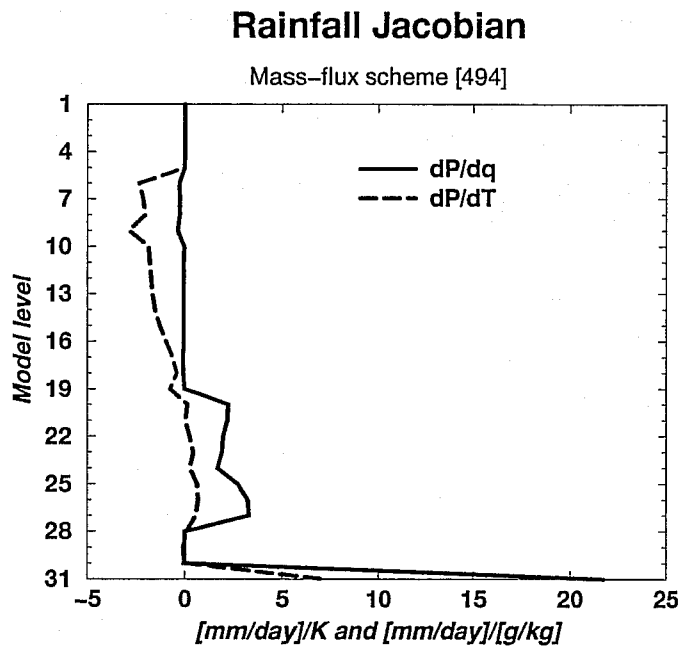

Figure 2: Jacobian vector of the sensitivity of surface rainfall rate P to modifications in temperature and specific humidity for the ECMWF mass-flux scheme applied on a tropical profile.

For the first-guess atmospheric profile selected in this study, the sensitivity of surface rainfall with respect to changes in temperature and specific humidity level by level is presented in Figure 2. This Jacobian vector has been computed in finite-differences using infinitesimal perturbations, corresponding to a regime where the tangent-linear approximation is valid. The convective cloud extends from level 27 up to level 6. A strong sensitivity is found near the surface for both temperature and moisture for the lowest model level, from which conditional instability is diagnosed and cloud properties defined to estimate CAPE. An increase by 1g/kg of specific humidity at that level enhances surface precipitation by 23 mm/day. In the lower part of the cloud, sensitivity to changes in water vapour dominates over changes in temperature. Whereas at higher levels (above the freezing level), the cooling of the atmospheric column represents the main mechanism by which surface precipitation can be increased.

When comparing these profiles with the vertical profiles of σ^b in Figure 1, it can be seen that the lower tropospheric moistening sensitivity also corresponds to a region where the forecast errors for specific humidity are rather large. Therefore, significant analysis increments are expected near level 26. In contrast, the large sensitivity of the convection scheme to changes in specific humidity near the surface corresponds to relatively low values of σ_q^b. The large analysis increments that convection could produce will be strongly reduced by the background term.

Results from two 1D-Var assimilations are shown on Figure 3 for $\alpha = 1.5$ and on Figure 4 for $\alpha = 0.5$. For an observed rainfall rate larger than the background, the convergence is very fast. After only three iterations the analysed rainfall rate has reached its optimal value, increasing from 30 mm/day to 42 mm/day. The minimization stops after 17 iterations when the norm of the gradient has decreased by 7 orders of magnitude. Increments of temperature and specific humidity at the end of the minimization show that moisture corrections dominate, with maximum values of 0.45 g/kg at level 25. The vertical structure of the increments reflects the background profile except near the surface where the Jacobian of the convection scheme is very large. Corrections in temperature are positive and maximum at the lowest model level corresponding to a destabilization of the profile and then become slightly negative as imposed by the vertical correlations of the background matrix. The relative humidity profile is increased with respect to the background value, mostly in regions where corrections in humidity are large and corrections in temperature negligible (between levels 27 and 20).

When the observed rainfall rate is lower than the background value (Figure 4) the minimization reaches a value close to the optimum value of 15 mm/day in 4 iterations (from the preconditioning) and stops after 13 iterations. However, the norm of the gradient has only decreased by 3 orders of magnitude which shows difficulties of the minimization process (presence of a threshold where the gradient is not defined). The vertical profile of increments shows almost a mirror picture of those produced with $\alpha = 1.5$ but with smaller amplitude. The maximum reduction in specific humidity is only 0.18 g/kg. The relatively strong warming of 0.1 K at level 23, in opposition to the Jacobian sensitivity at that level, is also a sign that the optimum found may be not unique. The analysed profile for relative humidity is almost unchanged with respect to the background, since increments are small and have compensating effects in the lowest model levels (cooling and drying).

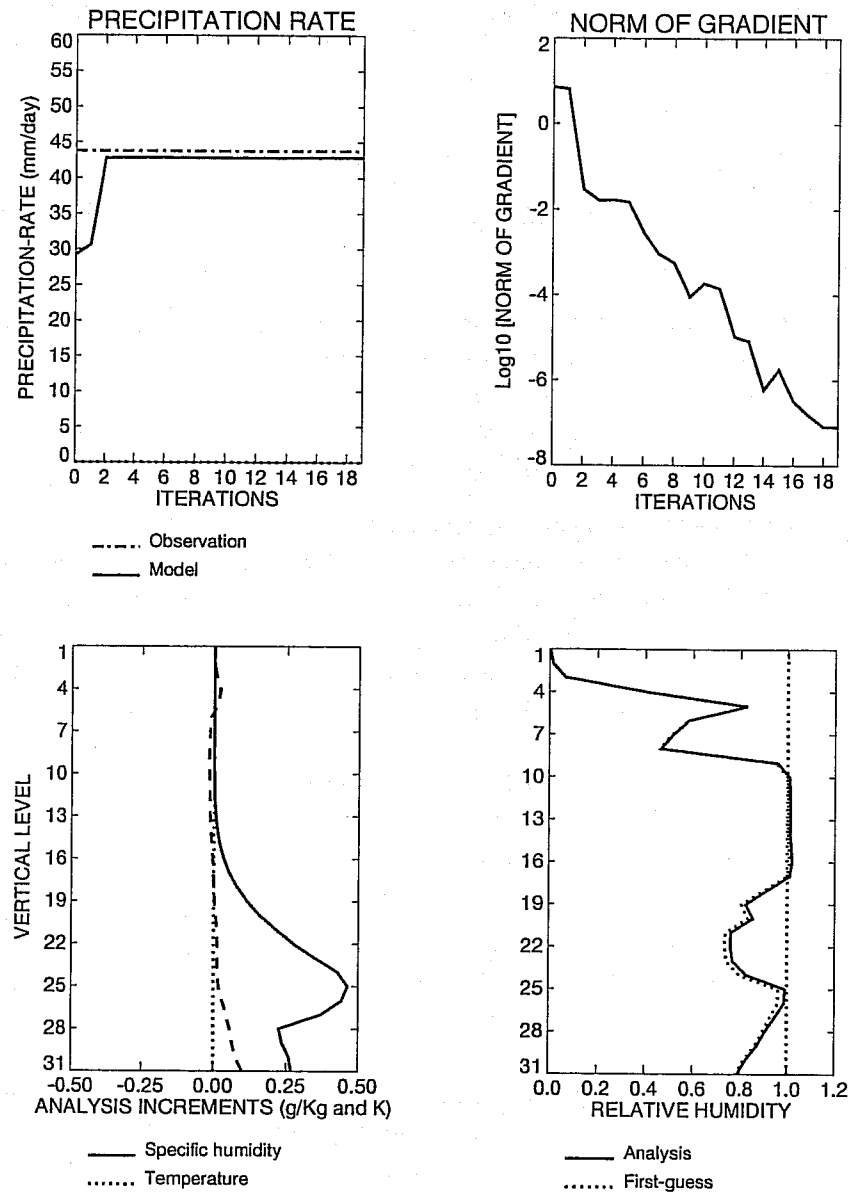

Figure 3: 1D-Var assimilation of rainfall rates (simulated observation 50% larger than the background value). The following quantities are plotted: precipitation rate at each iteration of the minimization with the observed value (upper left), norm of the gradient of the total cost-function in logarithmic scale (upper right), analysis increments for temperature and specific humidity (lower left) and vertical profiles of relative humidity for the first-guess and the analysis (lower right).

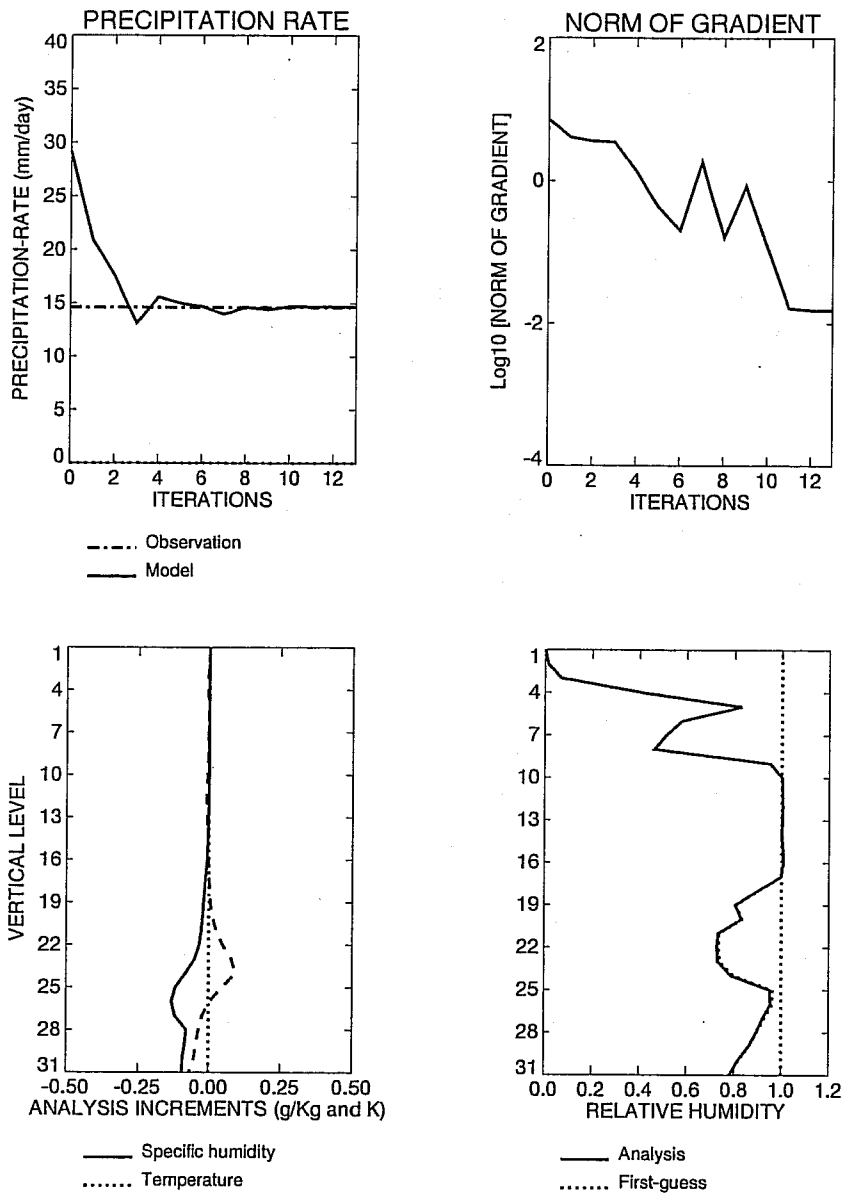

Figure 4: As Figure 3 but for an simulated observation of rainfall 50% lower than the background value

7. Assessment of TMI product accuracies

Since the TMI frequencies are almost the same as the SSM/I frequencies, with one more channel at 10.65 GHz, it is possible to assess their usefulness to derive total column water vapour, wind speed and cloud liquid water path within the 1D-Var assimilation described by *Phalippou* (1996) and run operationally at ECMWF since the end of February 1998.

The purpose of this section is therefore to provide the accuracy of products that can be derived from SSM/I and TMI for an inter-comparison study. The results obtained so far concern the total column water vapour (TCWV), the surface wind speed (WS) and the cloud liquid water path (LWP), as this assessment has already been done for the SSM/I radiometer at ECMWF (*Phalippou and Gérard*, 1996). The assessment of accuracy of the precipitation rate profiles derived from TMI will soon be done.

The results published in the literature give some indications about the accuracy of the SSM/I products. For instance the accuracies of SSM/I total column water vapour and marine ocean surface wind speed are quoted as 2.5 $kg.m^{-2}$ and 2 $m.s^{-1}$ respectively (see for instance *Alishouse et al.*, 1990; *Goodberlet and Swift*, 1992; *Petty*, 1990). The accuracy of SSM/I cloud liquid water path is more debatable due to the lack of ground truth for the validation, but it is estimated to lie within the range 0.02 and 0.05 $kg.m^{-2}$ (see *Greenwald et al.*, 1993 for instance).

A 1D-Var method has been developed at ECMWF for retrieving simultaneously TCWV, WS and LWP from SSM/I brightness temperatures over the oceans (*Phalippou*, 1996). The geophysical parameters are estimated simultaneously following the theory of non-linear optimal estimation (*Rodgers*, 1976) and are therefore the best set of parameters that explain the observed brightness temperatures while being consistent with the available 'a-priori' information provided by the ECMWF first guess.

This variational framework was used to infer the theoretical accuracies of the SSM/I 1D-Var products (*Phalippou and Gérard*, 1996) and has been adapted to the TMI radiometer characteristics. For this purpose, a preliminary computation of absorption coefficients for water vapour and oxygen to TMI frequencies has been necessary as inputs for the fast radiative transfer model. We summarize here the methodology and present the comparison study between SSM/I and TMI product accuracies.

TABLE 1. SSM/I SPATIAL RESOLUTION (EFOV) AND RADIOMETRIC ACCURACY (NEΔT).

Frequency (GHz)	19.35	22.235	37.0	85.5
Polarization	V & H	V	V & H	V & H
EFOV (km)	69 × 43	60 × 40	37 × 28	15 × 13
NEΔT (K)	0.8	0.8	0.6	1.1

TABLE 2. TMI SPATIAL RESOLUTION (EFOV) AND RADIOMETRIC ACCURACY (NEΔT).

Frequency (GHz)	10.65	19.35	21.30	37.00	85.50
Polarization	V & H	V & H	V	V & H	V & H
EFOV (km)	63 × 37	30 × 18	23 × 18	16 × 9	7 × 5
NEΔT (K)	0.63 V / 0.54 H	0.50 V / 0.47 H	0.71 V	0.36 V / 0.31 H	0.52 V / 0.93 H

7.1 Methodology

A by-product of the 1D-Var method is the estimation of the standard deviation of the 'a-posteriori' errors or 'theoretical accuracy' of the retrieved products. It can be shown (*Rodgers*, 1976) that the a posteriori error covariance matrix **A** of the estimation x can be approximated by:

$$\mathbf{A}(x) = [\mathbf{B}^{-1} + \mathbf{H}^{T}(x)\mathbf{R}^{-1}\mathbf{H}(x)]^{-1}$$

where **R** and **B** are the expected observation and background (or 'a-priori') error covariance matrices respectively. **H** is the linear observation operator obtained from the radiative transfer model which computes the brightness temperatures corresponding to the control variable x (i.e. its elements are the partial derivatives of the simulated brightness temperatures with respect to the control variable x). The control variable x is a 17 element vector which contains the natural logarithm of the specific humidity on 15 fixed pressure levels between 300 hPa and the surface, the surface wind speed and the cloud liquid water path derived from the first guess fields.

The 'a-posteriori error' variances of the estimate of x are given by the diagonal elements of **A**. In order to assess how much the observations improve the 'a-priori' knowledge, **A** must be compared to **B**. The improvement factor is defined as the ratio of the 'a-priori' to the 'a-posteriori' accuracy for each product. It is greater than or equal to 1. An improvement factor of 1 means that the 'a-priori' knowledge of this product has not been improved by the satellite measurements. The larger the ratio the better the improvement on the 'a-priori' knowledge of x.

7.2 Expected error covariance matrices

The so-called observation errors, defined in terms of brightness temperatures, include both measurement and radiative transfer model errors. They are assumed to be uncorrelated (i.e. the **R** matrix is diagonal). They are set to an approximate value of the measurements NeΔT's of the instruments (see Table 1 and Table 2) plus assumed errors in the radiative transfer model, namely 2 K for all the channels except for the 85.5 GHz channels where the errors are set to 3 K in order to account for the higher NeΔT's. In the case of TMI, the errors should be revised and could be set to 2 K for all the channels, as NeΔT at 85.5 GHz is lower than 1 K.

The error covariance matrix of the first guess specific humidity is the one used in the current SSM/I 1D-Var scheme at ECMWF. The upper left panel on Figure 5 shows the TCWV first guess errors computed on atmospheric profiles collected over one assimilation cycle, i.e. over a 6-hour period.

A 2 $m.s^{-1}$ first guess wind speed error has been assumed following the results of a comparison between ECMWF first guess wind field and ERS-1 scatterometer measurements (*Stoffelen and Anderson*, 1994).

There are several reasons to expect large errors in the first guess cloud liquid water path: there is a scale difference between the cloud represented in the ECMWF model and the SSM/I and TMI resolution, the time/space collocation between ECMWF cloud field and SSM/I and TMI measurements is particularly critical because some clouds have a large spatial/time variability, and finally the cloud field from the ECMWF model has not been extensively validated. Therefore the cloud liquid water path background error has been set to 0.2 $kg.m^{-2}$ which represents a weak constraint allowing the observations to mainly influence the retrieved cloud LWP.

7.3 Radiative transfer model

A detailed description of the radiative transfer model is given in *Phalippou* (1993; 1996). An overview is summarized here.

7.3 (a) Radiative transfer equation. The upwelling radiance R_{toa} at the top of the atmosphere is the sum of three terms:

$$R_{toa} = R_{up} + [\varepsilon_s B(T_s) + R_f]\tau_s$$

where R_{up} is the upwelling radiance due to the atmosphere alone, ε_s is the surface emissivity, B is the Planck function, T_s is the surface temperature, R_f is the radiance reflected by the surface at the surface level, τ_s is the transmittance from the ground to the top of the atmosphere. The ocean surface emissivity is described by the sea surface temperature and the 10-meter wind speed. The transmittance τ_s and the radiance R_{up} depend only on the atmospheric vertical profile of temperature, water vapour and cloud liquid water and on the incidence angle, assuming no precipitation or scattering from ice crystals.

7.3 (b) Atmospheric contribution. The atmosphere is divided into 40 pressure levels between 0.1 and 1000 hPa in order to integrate the radiative transfer equation. The background profile provided by the ECMWF first guess is interpolated from the original model levels on to the radiative transfer levels using a linear interpolation in pressure. The temperature and specific humidity values on the radiative transfer levels which are not covered by the model levels are set to the nearest model level values. The cloud liquid water is set to zero for the extrapolated radiative transfer levels.

The atmospheric absorption has been computed for each TMI and SSM/I channel according to the line-by-line model described by *Liebe* (1989) for the gas contribution (oxygen and water vapour), and from the Rayleigh scattering theory for the cloud droplets. The wind direction and Mie scattering by cloud and rain are not included in the radiative transfer model.

7.3 (c) Sea surface contribution. The emissivity/scattering of the sea surface, which depends on the dielectric properties of the surface, of the viewing geometry and of the polarization, has been computed using a geometric optics model. The roughness of the ocean as a function of wind speed has been derived from *Cox and Munk* (1954). A weighting of the slope as a function of the frequency has been used following the recommendations of *Hollinger* (1971) and *Wilheit* (1979). The sea foam contribution has been computed following *Stogryn* (1972) for the sea emissivity and *Monahan and O'Muircheartaigh* (1980) for the foam cover. The salinity of the ocean has been assumed to be constant (36 ppm).

7.4 Results

The 'a-posteriori' error and improvement factors have been computed from a large number of atmospheric and surface conditions for the SSM/I and TMI channel frequencies. Figure 5 shows the 'a-priori' and 'a-posteriori' TCWV errors, as well as the improvement factor on TCWV as a function of three parameters:. TCWV, WS and LWP. Figure 6 and Figure 7 show the results for WS and LWP respectively.

The improvement factor of TCWV computed from SSM/I characteristics ranges from 2 to 10 for values of TCWV from 5 to 70 $kg.m^{-2}$. For a TCWV equal to 40 $kg.m^{-2}$ for example, the TCWV 'a-priori' accuracy (background error) is about 15 $kg.m^{-2}$, and the 'a-posteriori' accuracy (analysis error) is about 1.79 $kg.m^{-2}$, which corresponds to an improvement factor of 8. The information extracted from SSM/I is equivalent to a measurement having an observation error of 1.80 $kg.m^{-2}$, which is less than the accuracies reported in the literature for the existing algorithms. For TMI the theoretical accuracy is better than for SSM/I; the improvement factor ranges from 2 to 13. In the previous example, the 'a-posteriori' accuracy on TCWV is about 1.3 $kg.m^{-2}$ for TMI versus 1.8 $kg.m^{-2}$ for SSM/I, which means that the information extracted from the microwave measurements is equivalent to a TCWV measurement with a 1.3 $kg.m^{-2}$ accuracy when TMI is used. The improvement factor obtained from the use of TMI is also better than the improvement factor obtained from SSM/I in any wind and cloud conditions as shown on the bottom panels of Figure 5. This general improvement is partly explained by the addition of the pair of low frequency channels in the TMI instrument. The fact that the TCWV accuracy is improved more significantly at high water vapour amounts suggests that the saturation of the brightness temperatures with TCWV is less important for the TMI water vapour absorption frequency (21.3 GHz) than for the SSM/I one (22.235 GHz).

The improvement factors of wind speed retrieved with SSM/I and TMI are better in windy conditions. With a 2 $m.s^{-1}$ background error, the wind speed 'a-posteriori' accuracy is 1.5 $m.s^{-1}$ and 1.3 $m.s^{-1}$ for SSM/I and TMI respectively for a wind speed of 7 $m.s^{-1}$. These errors are equivalent to the accuracies which would result from a minimum variance estimator using a 2 $m.s^{-1}$ background error and an independent wind speed estimate with a 2.3 $m.s^{-1}$ and 1.7 $m.s^{-1}$ accuracy for SSM/I and TMI respectively. Above 15 $m.s^{-1}$ it is suspected that the large improvement factor is due to an unrealistic modelling of the sea surface for high wind speed, which leads to an underestimation of the wind speed error. These high improvement situations occur under any humidity and cloud conditions, as shown with the isolated points on both bottom panels of Figure 6.

The LWP background error being set to 0.2 $kg.m^{-2}$, the theoretical LWP accuracies for SSM/I and TMI range between 0.01 and 0.07 $kg.m^{-2}$ depending on weather conditions as shown on the last three panels on Figure 7. The improvement factor is optimal in clear and dry conditions. Both instruments give similar improvement factors for LWP, which suggests that the addition of the pair of low frequency channels and the shift of the water vapour absorption frequency do not significantly improve the LWP 'a-posteriori' accuracy.

7.5 Conclusions on TMI products

There is potential for improving NWP model fields by using passive microwave radiances as they reduce the model background errors on TCWV, WS and LWP when included in the data assimilation system. The TMI radiometer is a better candidate than the SSM/I for providing an accurate total column water vapour and surface wind speed information, as the choice of the TMI frequencies helps to reduce the 'a-posteriori' error on these products.

The use of TCWV obtained from the SSM/I 1D-Var method in 4D-Var research assimilation experiments at ECMWF proved to be beneficial for the analysis and the forecast (*Gérard*, 1998) and has been operational at ECMWF since June 1998. A fortiori, TCWV data derived from TMI measurements could be used in the assimilation with more impact on the model fields, because these observations are proved to be more accurate than the observations provided by SSM/I.

The control variable of the radiative transfer model will be extended to include precipitation rate profiles, in order to assess the accuracy of the TMI retrieved products in rainy atmospheres. Scattering effects will be represented in a first step by the empirical formulation of extinction coefficients proposed by *Oslen et al.* (1978).

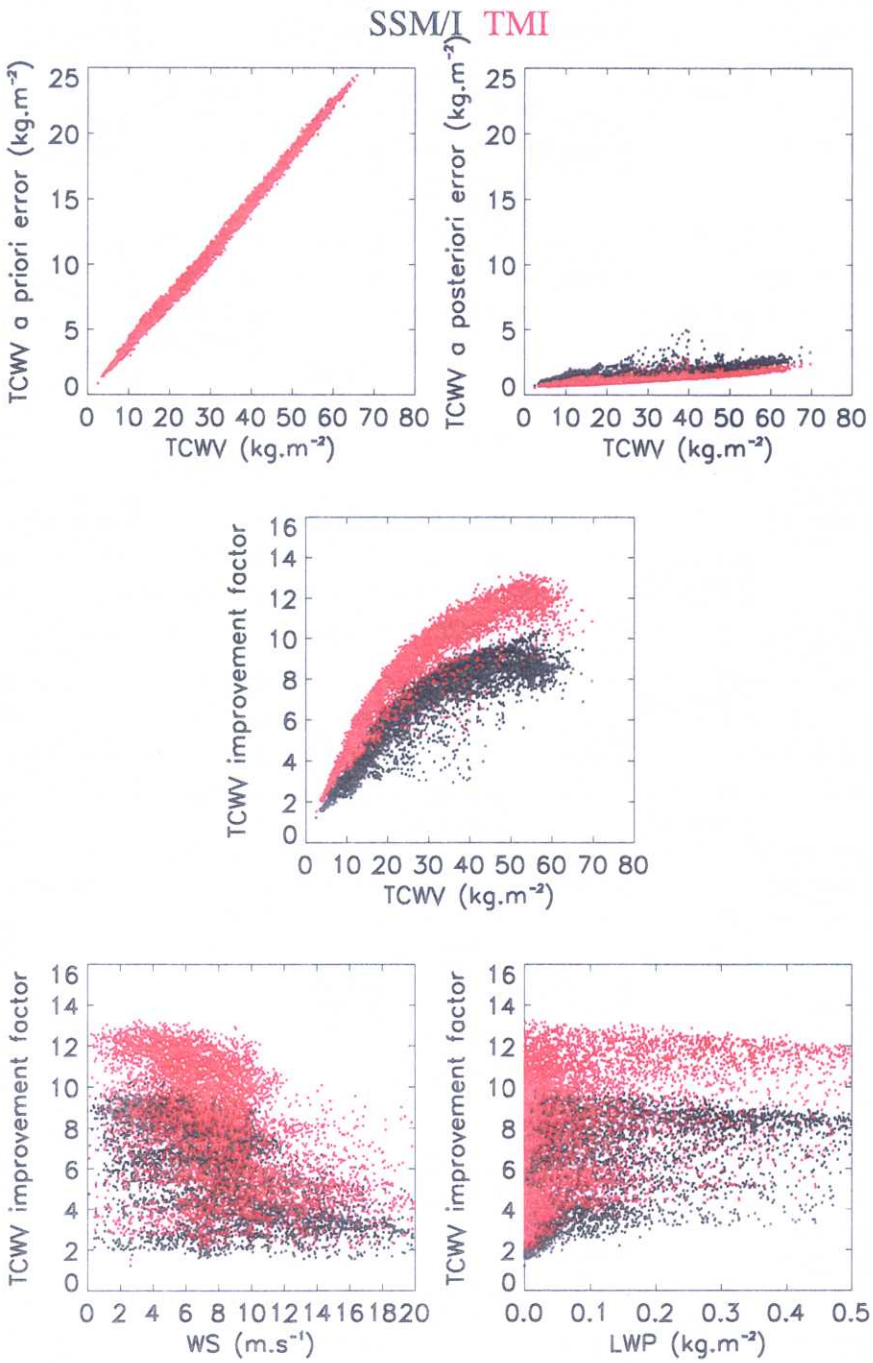

Figure 5: TCWV 'a-priori' error, TCWV 'a-posteriori' error (two top panels) and TCWV improvement factor as a function of TCWV values (middle panel), and as a function of the two other parameters (bottom panels). Black points for SSM/I, red points for TMI.

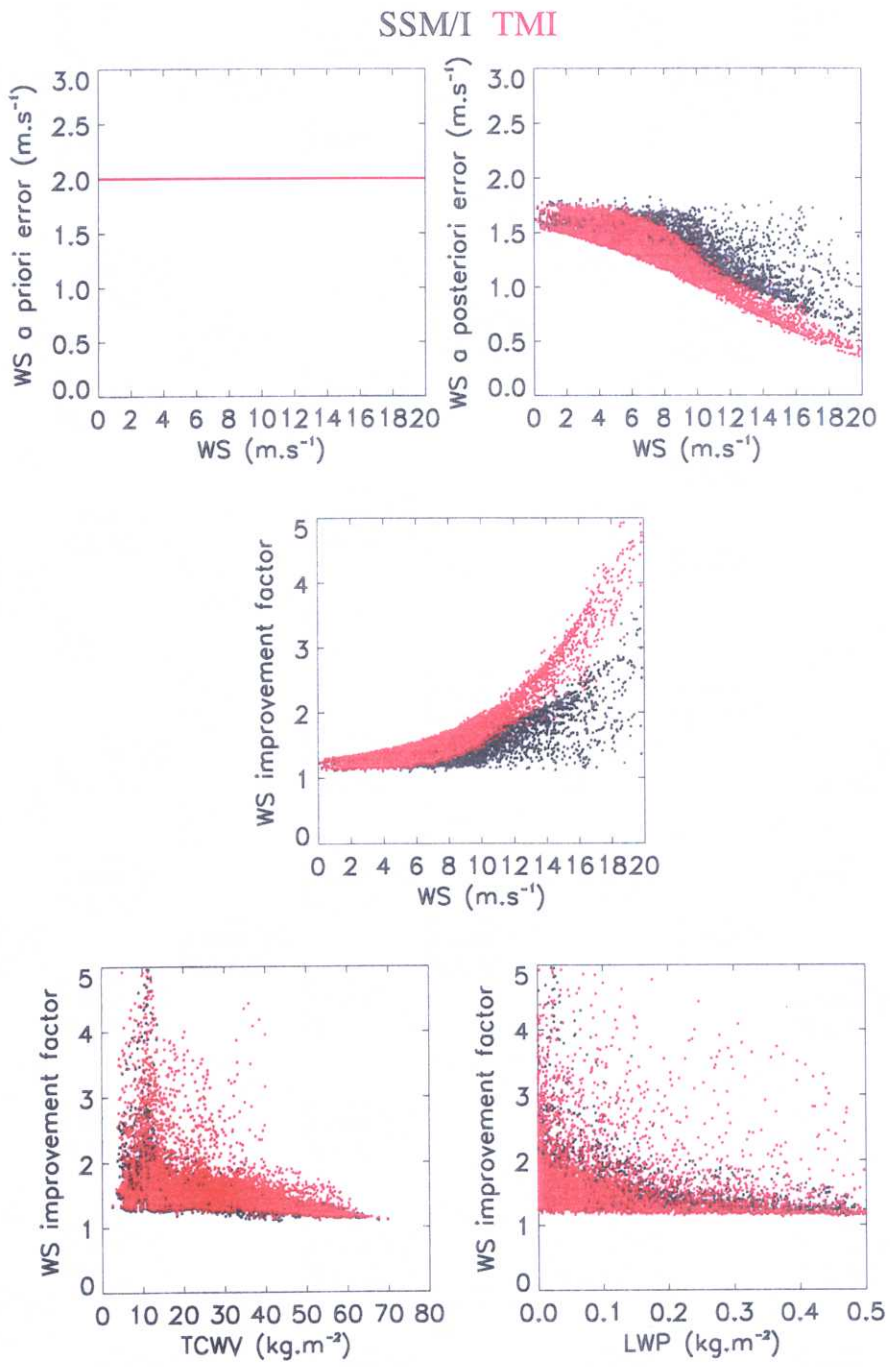

Figure 6: Same legend as Figure 5 but for WS

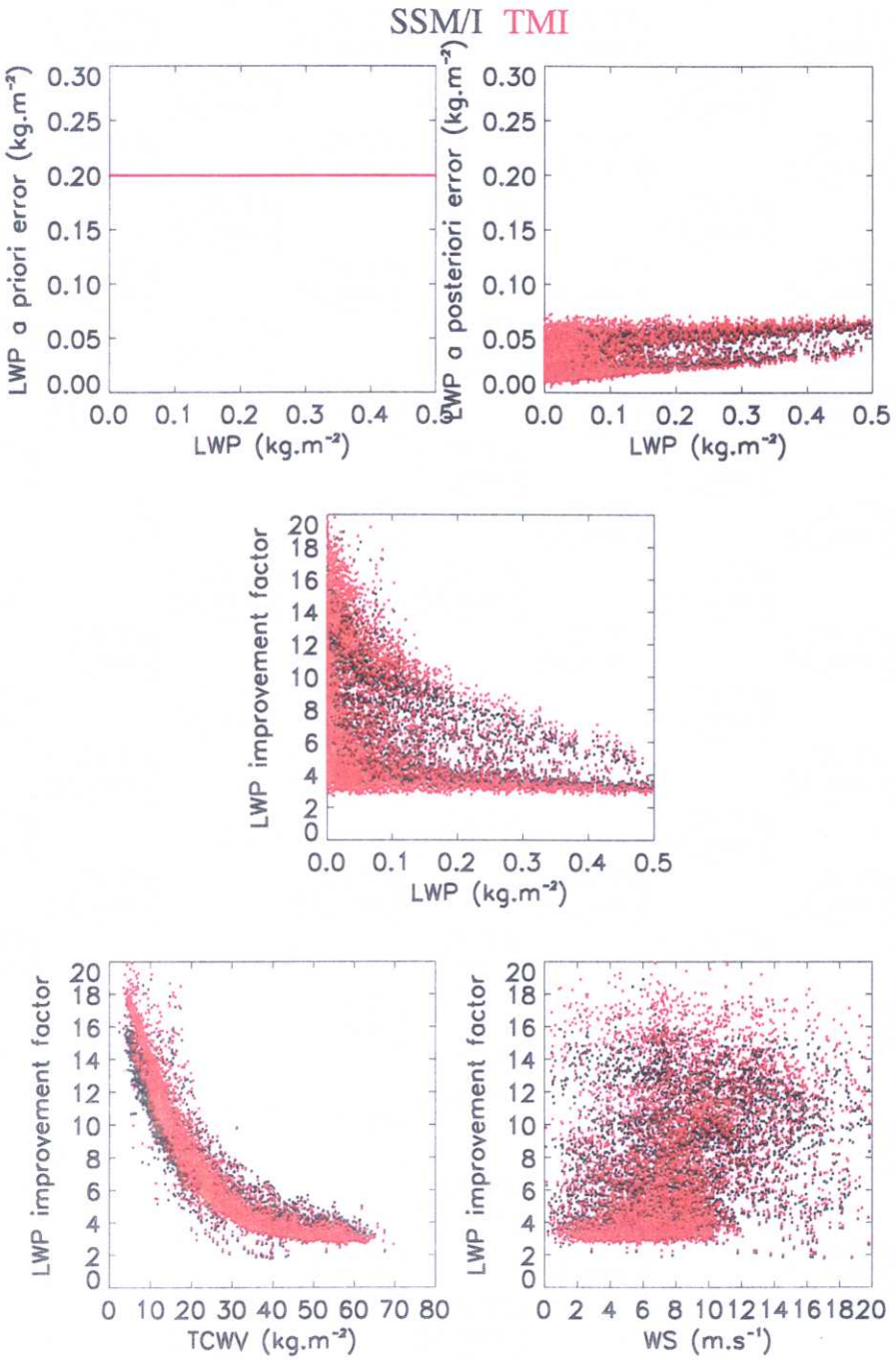

Figure 7: Same legend as Figure 5 but for LWP.

8. PRELIMINARY COMPARISON OF ECMWF AND SSM/I RAIN RATES

A first evaluation of the ECMWF first guess precipitation (6-hour forecast) against SSM/I derived precipitation rates from a statistical regression (*Ferraro*, 1997) is performed in this section. As an illustrative example the 18/04/1998 situation is selected, corresponding to the most recent operational version of the ECMWF model (including a linear grid with a T_L319 spectral resolution and an improved physical package, in particular the version of the deep cumulus convection scheme based on CAPE closure), and with maximum coverage of SSM/I data (about 300000 pixels every 6 hours).

A comparison of the two products (ECMWF first-guess and SSM/I derived rainfall rates) averaged at the same resolution ($1.5^o \times 1.5^o$) shows some similarities (Figure 8 and 9). The main areas of rather large precipitation rates (between 1 and 2 mm/hour) are consistent, even though the ECMWF model tends to produce broader patterns. In the ECMWF model, more areas with small rain rates (about 0.1 mm/hour) are present than in the SSM/I product. This maybe due to an inconsistency in the temporal sampling, since SSM/I are instantaneous estimates whereas the ECMWF products represent an average over a 6-hour window. On the other hand the detection of small rain rates is difficult by microwave technique since the signature can be equivalent to non-precipitating cloud liquid water. For example, an arbitrary threshold on liquid water path is set on the emission part of the Ferraro's algorithm to separate cloud water from rain water. Intense events, larger than 6 mm/hour, seen by SSM/I (even after a spatial averaging) on the 12 Z and 18 Z tracks, do not have any counterpart in the ECMWF model. This is likely to be a representativeness problem, and such observed points should be removed from the assimilation system by quality control checks.

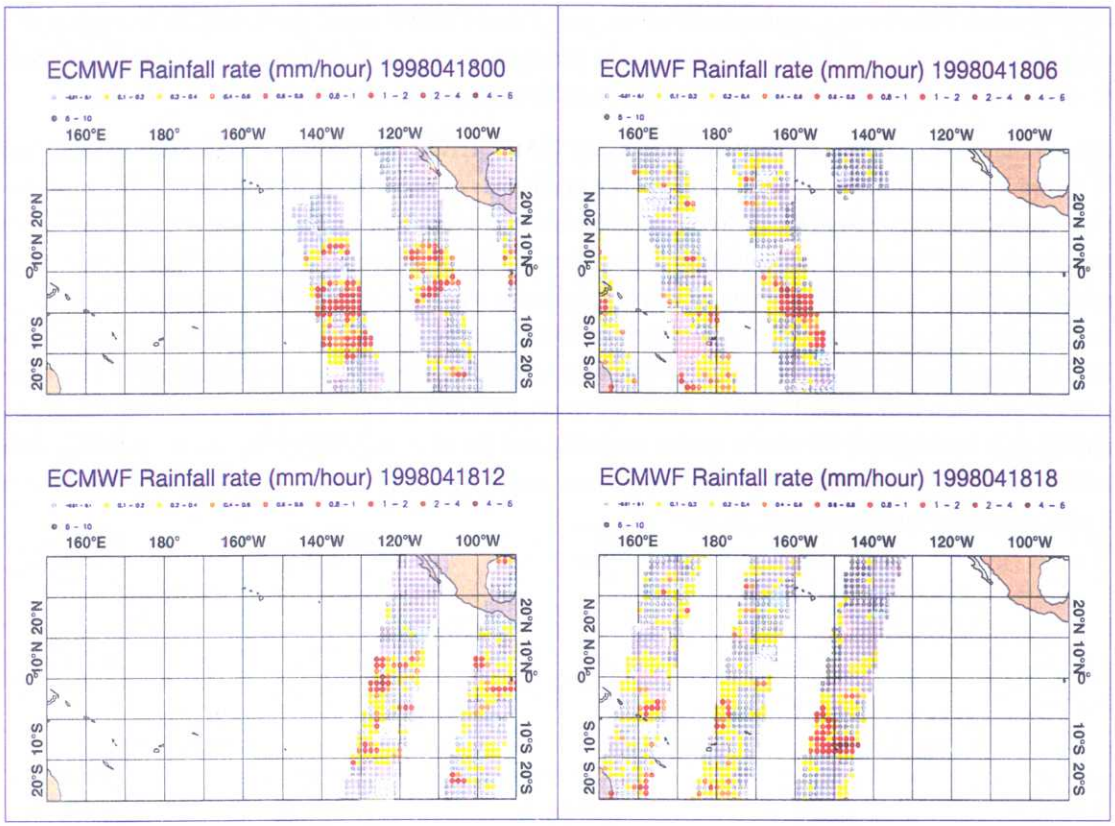

Figure 8: 6-hour accumulated precipitation from the operational ECMWF forecast model (T319L31) interpolated on a 1.5×1.5 degree grid along the swath of the SSM/I satellite on 18/04/1998 at 00, 06, 12 and 18 Z over the Eastern Equatorial Pacific.

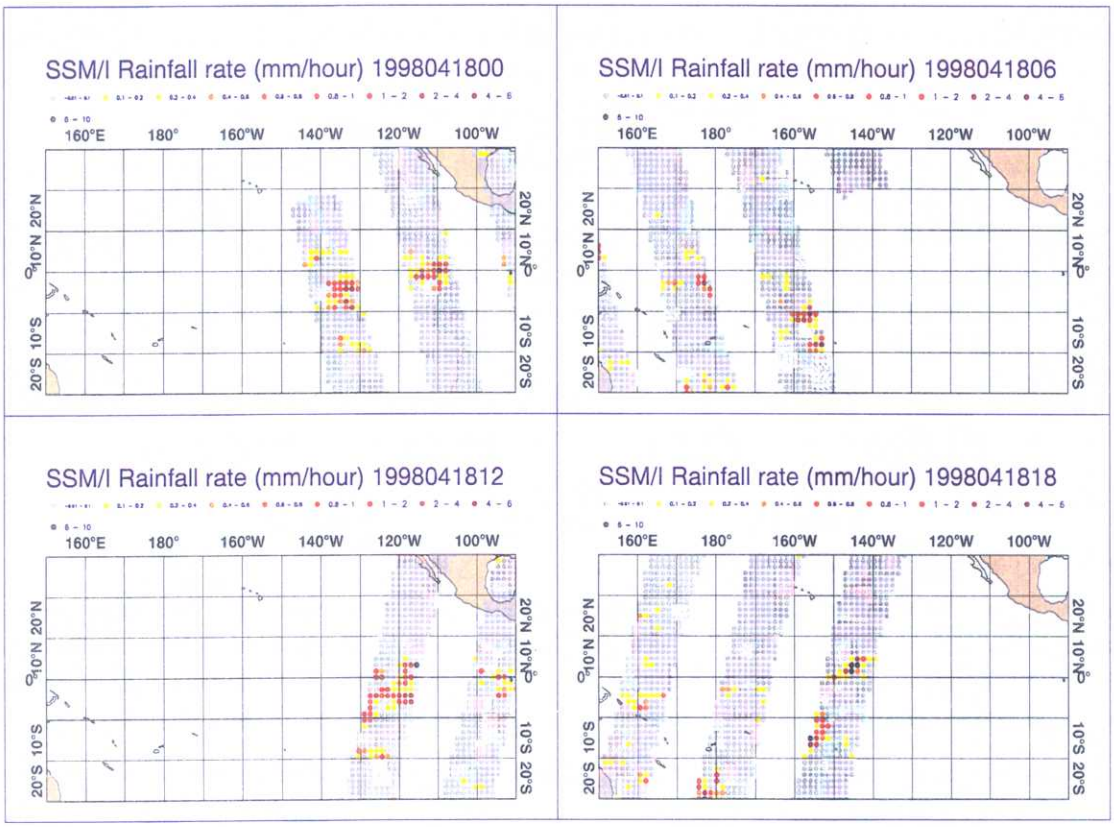

Figure 9: Instantaneous rainfall rates derived from a statistical regression using SSM/I brightness temperatures (Ferraro, 1997) on 18/04/1998 at 00,06,12 and 18 Z over the Eastern Equatorial

9. Recommendations

As shown in previous sections, the following spatial and temporal constraints are imposed by the current ECMWF 4D-Var data assimilation system:

> Horizontal resolution: 50 km (non-linear model at high resolution) and 150 km (adjoint model at low resolution)

> Vertical resolution: 500 m (31 levels)

> Sampling time: 1 hour

There are two different ways of using satellite measurements for data assimilation. The first one is to derive independently a 'satellite product' of a model quantity (e.g. model rainfall rate), and then use this product as an observation in the assimilation system. The second is to use satellite radiances as direct observations in the assimilation. This last approach requires an observation operator (radiative transfer model) to obtain the model counterpart of the satellite radiances. We propose to use both approaches for the assimilation of TRMM products in the ECMWF 4D-Var system.

Independent data will also be necessary to evaluate the quality of the analyses and of the medium-range weather forecasts issued from the 4D-Var system.

9.1 Assimilation of Level 1b data from TMI

Adapting the methodology developed for SSM/I, we plan to assimilate directly brightness temperatures (Tb's) from TMI within a 1D-Var algorithm for total column water vapour and surface wind speed (*Phalippou and Gérard*, 1996), as the accuracy assessment presented in Section 6 has shown a positive impact of the lower frequency channel and of the 22 GHz shift for these parameters. For this purpose, geolocated and calibrated Tb's need to be remapped for all channels on a common grid to apply the inversion algorithm. The local incidence angle at the Earth surface should be computed and attached to the Tb's. A surface type/height identifier should also be provided.

If these data can be made available in real-time (in November through TRMM Real-Time Data Service) an operational 4D-Var assimilation of TMI brightness temperatures could be possible very soon. A thinning of the Tb's will be required to reduce the amount of observations presented to the ECMWF data assimilation system. The current 125 km sampling used for SSM/I could be retained for TMI, even though in research mode the impact of higher resolution for Tb's could be evaluated. For these retrievals, the spatial sampling should not be too detrimental given the horizontal correlation scales of water vapour.

The Level 1b data will also be used for feasibility studies of 1D-Var assimilation of Tb's in rainy areas. In order to perform such studies, a scattering module should be added to the microwave radiative transfer model (and for its adjoint) and the profiles of hydrometeors produced by the moist physical parametrizations will need a precise evaluation.

9.2 Assimilation of TRMM precipitation rates

The high resolution of TMI (6 km to 50 km), VIRS (2 km) and PR (4 km) are not compatible with the current ECMWF model resolution. We suppose that the best product in terms of surface precipitation rates obtained by combining the four radiometers will be remapped on a common grid having a resolution between 15 and 20 km. We suggest obtaining the highest possible resolution and to interpolate this product on coarser grids at ECMWF for assimilation purposes.

It is recommended that the instantaneous surface precipitation rate is accompanied for each grid point by an estimate of its accuracy. A flag on the quality of the retrieved product could also be given (e.g. retrievals in the narrow swath should be of better quality). Information on sub-grid scale variability of rain rate within the grid box should be provided (variance, fractional coverage). An indicator on the type of precipitation (convective vs stratiform) would also be useful. As for brightness temperatures, the type of surface should be attached to the product (since it is likely that products over land are less reliable).

In the 4D-Var system the sampling time is not an important issue, and instantaneous rainfall rates can be assimilated in time-slots of one hour.

For research purposes, any format would be suitable (although the most suitable for our purposes is BUFR). Real-time data will most likely be provided in HDF format. Data can be converted at ECMWF in BUFR format before their introduction in the data assimilation system.

These data should be provided for two periods of 2 or 3 weeks in order to perform assimilation cycles and medium range forecasts, and evaluate the significance of improvements coming from the assimilation of rainfall rates. These periods should be chosen during the TRMM validation field experiments when additional observations are available to allow independent validation of ECMWF analyses and forecasts.

9.3 Evaluation of analyses and forecasts

In addition to the standard diagnostics performed at ECMWF to evaluate the skill of operational analyses and forecasts, we propose to use available data from TRMM validation field campaigns. These data would be independent measurements of precipitation from ground based meteorological radars, and from the PR in terms of vertical profiles (including rain occurrence, water phase, height of the melting layer). Airborne dual beam Doppler radar data could provide vertical

profiles of convective source terms, surface wind in rainy areas and 3D wind field structure. These data should be made available at the scale of measurements (compatible with a model grid box) for selected cases (e.g. tropical cyclone, tropical squall line, mesoscale convective systems) during field campaigns. Conventional measurements should also be made available for validation purposes (rain gauges, radiosondes, surface fluxes,...). In-situ microphysical airborne measurements on cloud and rain ice properties (concentrations, fallout,...) would help to improve the physical parametrizations of moist processes in the ECMWF model. Surface latent heat fluxes deduced from TMI and VIRS by the University of Munich can be used to evaluate the description of the tropical boundary layer, which is an important issue for the initiation of convection and precipitation evaporation. The assimilation of such data in the 4D-Var system could be possible in principle, but would require important developments outside the scope of the present program. The improved surface emissivity model developed at UCL could be used in the ECMWF microwave radiative transfer model. For all the required data sets presented above, accuracy should also be provided.

ACKNOWLEDGEMENTS

The authors are grateful to Adrian Simmons and Anthony Hollingsworth for their comments and suggestions. Thanks are also due to Jacques Testud (CETP) and Pedro Poiares Baptista (ESTEC) for the scientific coordination of the EuroTRMM programme. This work was partly supported by EU Contract No ENV4-CT97-0421 (DG12-VOMA) and ESA/ESTEC Contract No 12651/97/NL/NB.

APPENDIX A SUMMARY OF USER REQUIREMENTS

Required product	Spatial resolution	Temporal resolution	Model purpose	Spatial resolution	Temporal resolution
TMI calibrated brightness temperatures > Geolocation > Surface type > Local incidence angle > Accuracy	Common grid (~15 km) Global coverage	Instantaneous data in real time *TRMM Real-Time Data Service*	1D-Var / 4D-Var assimilation of Tb's for total water vapour column and surface wind speed retrievals (operational) 1D-Var / 4D-Var assimilation of Tb's in rainy areas (research)	100 km (sampled)	Hourly model products
Surface precipitation (derived from TMI, PR, VIRS data) > Geolocation > Surface type > Quality flag > Accuracy > Precipitation type > Sub-grid scale variability (fractional coverage, variance) > Vertical extent	Common grid (~15 km) Global coverage	Instantaneous data for 15 days 2 periods during field experiments *CETP-FMA-DLR*	1D-Var / 4D-Var assimilation of satellite-derived rainfall rates (feasibility studies for future operational applications)	50-150 km (averaged)	Hourly model products

TABLE 3. REQUIREMENTS FOR ASSIMILATION PURPOSES

Type of data	Spatial resolution	Temporal resolution	Model purpose	Spatial resolution	Temporal resolution
> TRMM PR (mm/hour + dBZ)	Δx=4 km Δz=250 m Field experiments	Special events during field experiments *CETP*	Evaluation of model rain rate profiles (rain occurrence, water phase, melting layer height),	Vertical cross sections Δz= 500 m Horizontal scale of the systems under consideration	Instantaneous model outputs
> Dual beam airborne radar	Δx=1 km Δz=500 m Field experiments	Special events during field experiments *CETP*	Evaluation of model 3D-wind structure and vertical profiles of convective source terms	Grid box averages (15 to 50 km) Δz=500m	Instantaneous model outputs
> Ground based radar	Δx=1 km Δz=500 m	Hourly data (15 days) *RAL-UE*	Evaluation of model hydrometeors profiles	Grid box averages (15 to 50 km) Δz=500 m	Hourly model outputs
> Retrieved surface latent heat fluxes from TMI and VIRS > Geolocation > Accuracy	Δx=15 km Global coverage	Hourly data (15 days) *UM*	Evaluation of model latent heat fluxes at the surface	15 to 50 km	Hourly and daily model products

TABLE 4. REQUIREMENTS FOR VALIDATION PURPOSES

APPENDIX B THE ADJOINT TECHNIQUE FOR 1D-VAR ASSIMILATION

Given an observation y_0 of a physical quantity (satellite radiance, precipitation flux, radiative flux), a non-linear operator H provides the model counterpart y of the observation from an atmospheric profile x.

$$y = H(x)$$

This non-linear operator which projects the model variable in the observation space can be for example a physical parametrization (if the observation is a rainfall rate), a radiative transfer model (if the observation is a satellite radiance) or a spatial interpolation operator.

The tangent-linear operator of H, noted $\mathbf{H}$, provides the change δy of the physical parameter y to an infinitesimal perturbation of the model input δx. Thus:

$$\delta y = \mathbf{H}(\delta x)$$

The tangent linear operator can be written in a matrix form (Jacobian) which expresses the partial derivatives of the variable y with respect to the input vector x:

$$\mathbf{H}_{ij} = \frac{\partial y_i}{\partial x_j}$$

The index i goes from 1 to M (dimension of y) and the index j goes from 1 to N (dimension of x).

$$\delta y_i = \sum_{j=1}^{N} \frac{\partial y_i}{\partial x_j} \cdot \delta x_j$$

The 1D-Var problem consist in minimizing a cost-function which represents the model departure from a given observation through a modification of the atmospheric profile.

$$J_o(x) = \frac{1}{2}(y - y_o)^T \mathbf{R}^{-1}(y - y_o)$$

where $\mathbf{R}$ is the covariances matrix of observation errors.

The minimization requires the gradient of the cost-function with respect to x to be known in a classical descent algorithm (steepest descent, conjugate gradient, quasi-newton).

The gradient of the cost-function with respect to y is easy to estimate:

$$\nabla_y J_0 = \mathbf{R}^{-1}(y - y_o)$$

The gradient with respect to x can be expressed using chain rule derivatives and $\nabla_y J_o$:

$$\cdot \frac{\partial J_o}{\partial x_i} = \sum_{j=1}^{M} \frac{\partial y_j}{\partial x_i} \cdot \frac{\partial J_0}{\partial y_j}$$

The index i goes from 1 to N (dimension of $\nabla_x J_o$) and the index j goes from 1 to M (dimension of $\nabla_y J_o$).

The gradient of the cost-function with respect to x (input variable) can be expressed from the knowledge of its gradient with respect to y (output variable) via the following linear operator:

$$\mathbf{H}_{ij}^{T} = \frac{\partial y_j}{\partial x_i}$$

This operator is the transpose (adjoint) of the tangent-linear operator $\mathbf{H}$

Finally:

$$\nabla_x J_o = \mathbf{H}^T(\nabla_y J_o)$$

This technique is an efficient way to get the gradient of a cost-function with respect to the input variables when the dimension of the control variable is large.

APPENDIX C LIST OF ACRONYMS

•BUFR: Binary Universal Form for the Representation of meteorological data

•CAPE: Convective Available Potential Energy

•CETP: Centre d'Etude des Environnements Terrestres et Planétaires

•DLR: German Aerospace Research Institute

•ECMWF: European Centre for Medium-range Weather Forecasts

•EFOV: Effective Field Of View

•FMA: Fondazione per la Meteorologia Applicata

•FSU: Florida State University

•GOES: Geostationary Operational Environmental Satellite

•HDF:Hierarchical Data Format

•HIRS: High-resolution Infrared Radiation Sounder

•INRIA: Institut National de Recherches en Informatique Appliquée

•LWP: Liquid Water Path

•MPI: Max-Planck Institute for Meteorology

•NCEP: National Centers for Environmental Prediction

•NMC: National Meteorological Center

•NW : Numerical Weather Prediction

•PR: Precipitation Radar

•RA : Rutherford Appleton Laboratory

•SSM/I: Special Sensor Microwave/Imager

•TMI: TRMM Microwave Imager

•TOVS: TIROS Operational Vertical Sounder

•TCWV: Total Column Water Vapour

•TRMM: Tropical Rainfall Measuring Mission

•UCL: Université Catholique de Louvain-la-Neuve

•UE: University of Essex

•UM: University of Munich

•VIRS: Visible and Infrared Radiometer System

•WS: Wind Speed

•1D-Var: One-dimensional Variational analysis

•4D-Var: Four-dimensional Variational analysis

REFERENCES :

Alishouse, J. C., S. A. Snyder, J. Vongsathorn and R. R. Ferraro, 1990: Determination of oceanic precipitable water from the SSM/I. *IEEE Trans. Geosci. Remote Sensing*, **28**, 811-816.

Andersson, E., J. Pailleux, J.R. Eyre, A.P. McNally, G.A. Kelly, P. Courtier and F. Rabier, 1993: Assimilation of satellite data by 3D-Var at ECMWF. *Proceedings of the 1993 ECMWF Seminar*, 167-188.

Aonashi, K., K. Kuma and Y. Matsushita, 1997 : A physical initialization method for the Economical Prognostic Arakawa-Schubert scheme. *J. Meteor. Soc. Japan*, **75**, 597-618.

Bouttier, F., J. Derber and M. Fisher, 1997: The 1997 revision of the J_b term in 3D/4D-Var. ECMWF *Tech. Memo No 238.*

Courtier, P., C. Freydier, J.-F. Geleyn, F. Rabier, and M. Rochas, 1991: The ARPEGE project at Météo-France. P*roceedings of the 1991 ECMWF Seminar on Numerical Methods in Atmospheric Models, Vol. II*, 192-231.

Courtier, P., J.-N. Thépaut and A. Hollingsworth, 1994: A strategy for operational implementation of 4D-Var using an incremental approach. *Q.J. R. Meteorol. Soc.*, **120**, 1367-1388.

Cox, C. and W. Munk, 1954: Measurements of the roughness of the sea surface from photographs of the sun's glitter. *J. Opt. Soc. Amer.*, **44**, No 11, 838-850.

Errico, R.M. and P.J. Rasch, 1988: A comparison of various normal-mode initialization schemes and the inclusion of diabatic processes. *Tellus*, **40A**, 1-25.

Ferraro, R R, 1997: Special sensor microwave image derived global rainfall estimates for climatological applications. *J. Geophys. Res.*, **102**, 16715-16735.

Fillion, L. and R. Errico, 1997: Variational assimilation of precipitation data using moist convective parameterization schemes: A 1D-Var study. *Mon. Weather. Rev.*, **125**, 2917-2942.

Gérard, É., 1998: Assimilation of SSM/I 1DVAR Total Column Water Vapour in 4DVAR. *Research Department Memorandum*, ECMWF, UK, R43/EG/33, 29 Apr. 1998.

Gilbert, J.-C. and C. Lemaréchal, 1989: Some numerical experiments with variable-storage quasi-Newton algorithms. *Mathematical Programming*, **B25**, 407-435.

Goodberlet, M. A. and C. T. Swift, 1992: Improved retrievals from the DMSP wind speed algorithm under adverse weather conditions. *IEEE Trans. Geosci. Remote Sensing*, **30**, No 5, 1076-1077.

Greenwald, T. J., G. L. Stephens, T. H. Vonder Haar and D. L. Jackson, 1993: A physical retrieval of cloud liquid water over the global oceans using the Special Sensor Microwave/Imager observations. *J. Geophys. Res.*, **98**, D10, 18471-18488.

Heckley, W.A., G. Kelly and M. Tiedtke, 1990: On the use of satellite-derived heating rates for data assimilation within the tropics. *Mon. Weather Rev.*, **118**, 1743-1757.

Hollinger, J. P., 1971: Passive microwave measurements of sea surface roughness. *IEEE Trans. Geosci. Electron.*, **9**, No 3, 165-169.

Jakob, C. and S.A. Klein, 1998 : The role of vertically varying cloud fraction in the parametrization of microphysical processes in the ECMWF model. *ECMWF Tech. Memo No 251.*

Krishnamurti, T.N., K. Ingles, S. Cooke, T. Kitade and R. Pasch, 1984: Details of low-latitude, medium-range numerical weather prediction using a global spectral model. Part 2: Effects of orography and physical initialization. *J. Meteor. Soc. Japan*, **62**, 613-648

Krishnamurti, T.N., H.S. Bedi, W. Heckley and K. Ingles, 1988: Reduction of spinup time for evaporation and precipitation in a spectral model. *Mon. Weather Rev.*, **116**, 907-920.

Krishnamurti, T.N., J. Xue, H.S. Bedi, K. Ingles and D. Oosterhof, 1991: Physical initialization for numerical weather prediction over the tropics, *Tellus*, **43A**, 53-81.

Krishnamurti, T.N., H.S. Bedi and K. Ingles, 1993: Physical initialization using SSM/I rain rates. *Tellus*, **45A**, 247-269.

Liebe, H. J., 1989: MPM - an atmospheric millimetre wave propagation model. *Int. J. Infrared and Millimetre Waves*, **10**, No 6, 631-650.

Monahan, E. C. and I. O. Muircheartaigh, 1980: Optimal power-law description of oceanic whitecap coverage dependence on wind speed. *J. Phys. Oceanogr.*, **10**, 2094-2099.

Olsen, R.L., D.V. Rodgers, and D.B. Hodge, 1978: The aR^b relation in the calculation of rain attenuation. *IEEE Trans. Antennas Propag.*, **AP-26**, 318-328.

Parrish , D.F. and J.C. Derber, 1992: The National Meteorological Center's Spectral Statistical Interpolation Analysis System. *Mon. Weather Rev.*, **120**, 1747-1763.

Petty, G. W., 1990: On the response of the special sensor microwave/imager to the marine environment - Implications for atmospheric parameter retrievals. *PhD dissertation*, Univ. of Washington, 291 pp.

Phalippou, L., 1993: A microwave radiative transfer model. *ECMWF Tech. Memo. No. 190.*

Phalippou, L., 1996: Variational retrieval of humidity profile, wind speed and cloud liquid water path with the SSM/I: Potential for numerical weather prediction. *Q. J. R. Meteorol. Soc.*, **122**, 327-355.

Phalippou, L. and É. Gérard, 1996: Use of precise microwave imagery in Numerical Weather Prediction. *Study report to the European Space Agency*, 70 pp [Available from ECMWF].

Puri, K. and M.J. Miller, 1990: The use of satellite data in the specification of convective heating for diabatic initialization and moisture adjustment in numerical weather prediction models. *Mon. Weather Rev.*, **118**, 67-93

Rabier F., A. McNally, E. Andersson, P. Courtier, P. Unden, J. Eyre, A. Hollingsworth and F. Bouttier, 1997a The ECMWF implementation of three dimensional variational assimilation (3D-Var). Part II: Structure functions. *ECMWF Tech. Memo. No 242.*

Rabier, F, J-F Mahfouf, M Fisher, H Jarvinen, A Simmons, E Andersson, F Bouttier, P Courtier, M Hamrud, J Haseler, A Hollingsworth, L Isaksen, E Klinker, S Saarinen, C Temperton, J-N Thépaut, P Unden and D Vasiljevic, 1997b: Recent experimentation on 4D-Var and first results from a Simplified Kalman Filter. *ECMWF Research Department Technical Memorandum No. 240*, 42 pp.

Rodgers, C. D., 1976: Retrieval of atmospheric temperature and composition from remote sensing of thermal radiation. *Rev. Geophys. Space Phys.*, **14**, 609-624.

Simmons, A.J and D.M Burridge, 1981: An energy and angular-momentum conserving vertical finite-difference scheme and hybrid vertical coordinates. *Mon. Weather Rev.*, **109**, 758-766

Simpson, J., C. Kummerow, W.-K. Tao and R.F. Adler, 1996: On the Tropical Rainfall Measuring Mission (TRMM). *Meteor. Atmos. Phys.*, **60**, 19-36

Stoffelen, A. and D. Anderson, 1994: The ECMWF contribution to the characterisation, interpretation, calibration and validation of ERS-1 scatterometer backscatter measurements and winds, and their use in numerical weather prediction models. *Final Report, ESA contract 9097/90/NL/BI.*

Stogryn, A., 1972: The emissivity of sea foam at microwave frequencies. *J. Geophys. Res.*, **77**, No 9, 1658-1666.

Sundqvist, H., 1988: Parameterization of condensation and associated clouds in models for weather prediction and general circulation simulation. *Physically-Based Modelling and Simulation of Climate and Climate Change*, M.E. Schlesinger, Ed. Kluwer, 433-461

Tiedtke, M., 1989: A comprehensive mass flux scheme for cumulus parameterization in large-scale models. *Mon. Weather. Rev.*, **117**, 1779-1800.

Tiedtke, M., 1993: Representation of clouds in large-scale models. *Mon. Weather. Rev.*, **121**, 3040-3061

Treadon, R.E., 1997: Assimilation of satellite derived precipitation estimates with the NCEP GDAS. *Ph.D. Dissertation, Florida State University*, 348 pp.

Wilheit, T. T., 1979: A model for the microwave emissivity of the ocean's surface as a function of wind speed. *IEEE Trans. Geosci. Electron.*, GE-**17**, No 4, 244-249.